Report on a problem studied at the UK Mathematics-in-Medicine Study Group Nottingham 2000
< https://mmsg.mathmos.net/uk/2000/tumour-drug/ >

Effect of Fibrinogen E-fragment on Tumour Growth

Chris Breward, Claire Lewis, University of Sheffield Medical School
Helen Byrne, Eleanor Clark, Peter Howell, John King, David Gammack,
Jonathan Wattis, Duncan Wilson, University of Nottingham
Peter Kramer, Rensselaer Polytechnic Institute
John Billingham, Andy King, University of Birmingham
Jon Chapman, John Norbury, University of Oxford
Markus Owen, University of Loughborough
Marcus Tindall, Colin Please, University of Southampton

February 2001

Introduction

Angiogenesis, the development of new blood vessels from the existing vasculature, is a complex process involving degradation of the matrix round each vessel and then the migration, proliferation and differentiation (rounding up) of endothelial cells to form new vessels. These steps usually occur in response to increased production by local cells of such pro-angiogenic cytokines as vascular endothelial growth factor (VEGF) and basis fibroblast growth factor (bFGF) which bind to specific receptors on endothelial cells to activate them. The finding that angiogenesis is critical to the growth of tumours beyond about 2 mm^3 in size (as well as the progression of such diseases as rheumatoid arthritis, psoriasis and blindness in diabetes) has prompted the widespread hunt for angiogensis inhibitors. Ideally, this new class of drug should be specific for (proliferating) blood vessels engaged in angiogenesis, and should leave (quiescent) blood vessels in healthy tissues unharmed. Prof. Claire Lewis believes that her research group have now developed such a drug: a fragment of the naturally-occurring protein, fibrinogen.

Fibrinogen is a key component of the clotting cascade that can be cleaved into various fragments *in vivo* by the enzymes thrombin and plasmin. Results obtained by Prof Lewis' group show that a 50kDa polypeptide, formed by plasmin cleavage of fibrinogen and called fibrinogen E-fragment (FgnE), markedly reduces VEGF- and bFGF- stimulated migration and differentiation of human endothelial cells *in vitro*. By contrast FgnE has virtually no effect on human endothelial cells in the absence of VEGF or bFGF.

FgnE has also produced potent anti-angiogenic effects *in vivo*, in animal models. Daily injections of FgnE into tumour-bearing mice for 10 days markedly suppressed tumour growth compared to control animals injected with the same volume of an "inert liquid", see Figure 1. It also resulted in widespread damage to endothelial cells lining blood vessels, intravascular thrombosis (ie massive clotting in the vessels) and tumour cell necrosis at the centre of the tumours, see Figure 2. No such effects were seen at the edge of the tumours (or in the lungs, liver or kidneys) of FgnE-treated mice, suggesting that the anti-angiogenic effects of FgnE were restricted to tumour blood vessels. The effect at the centre of the tumour was sufficient to cause a

Figure 1: Graph showing the tumour volume up to 10 days after injection of drug, for control tumours (upper line) and treated tumours (lower line).

Figure 2: Schematic of the structure of treated tumours after 10 days

significant reduction in tumour volume over 10 days of treatment: as the blood vessels became occluded, tumour cells surrounding these vessels were starved of nutrients and died. Macrophages then migrated into these necrotic areas and phagocytosed (*i.e.* removed) the cell debris.

For the drug to be fully effective in the treatment of human tumours, it is important to understand why blood vessels at the edge of the tumour do not appear to be adversely affected by the drug. There is no evidence, to date, that these outer blood vessels are non-angiogenic (ie quiescent), like blood vessels in healthy tissues or that they carry blood less effectively than vessels in the centre of the tumour. As a result, the blood-borne drug should act equally on all blood vessels within the tumour. The aim of this report is to use mathematical techniques in order to investigate the possible differences between the outer and inner architecture of the tumours with regard to drug access to the vessel surface and anti-angiogenic efficacy *in vivo*.

Interpretation and Modelling Aims

The key features of the experimental results presented in Figures 1,2 are listed below.

- The volume of the control tumour increases approximately linearly over the first ten day period of the experiments;
- Treated tumours are smaller than untreated tumours;

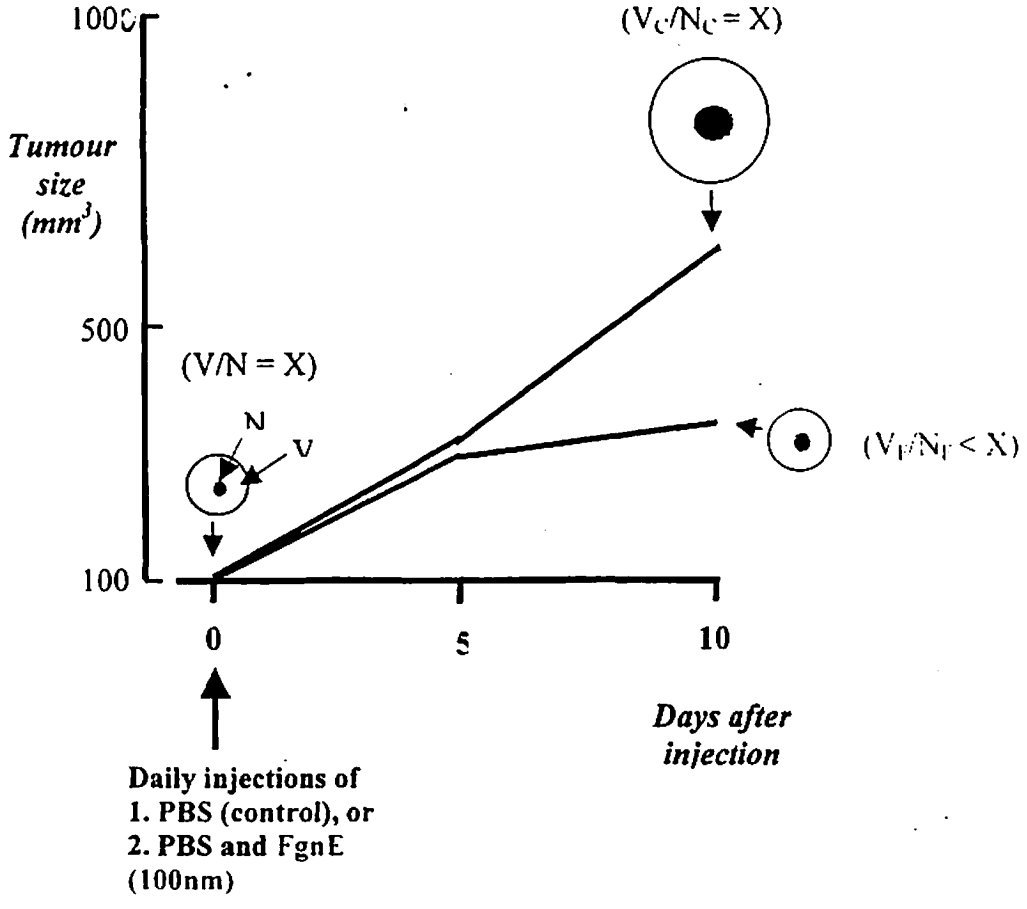

Figure 1 : Graph showing the tumour volume up to 10 days after injection of drug, for control tumours (upper line) and treated tumours (lower line).

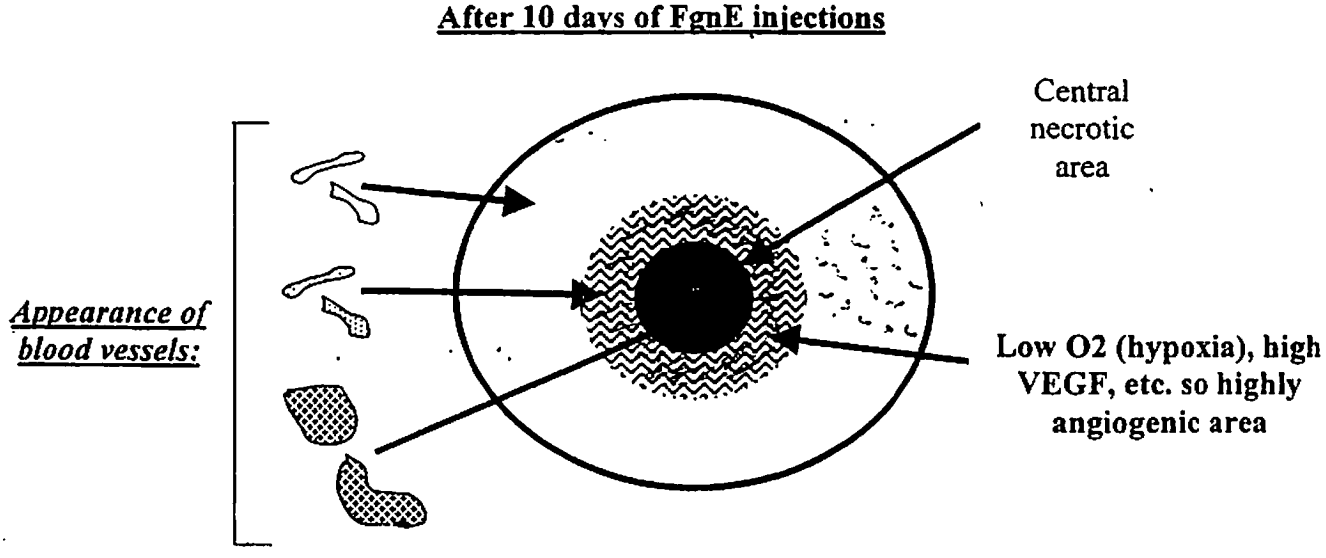

Figure 2 : Schematic of the structure of treated tumours after 10 days

- Both the control and treated tumours consist of a central necrotic region and an outer region of "healthy" tumour cells;
- The vascular density in the perfused (or viable) region of the tumur remains constant over time (in both the control and treated tumours). There are no patches of necrosis in the outer viable rime;
- The drug causes blood vessels near the necrotic region to fill with fibrinogen. Some vessels appear swollen or dilated compared to those in the viable part of the tumour (and in the hypoxic part of the control);
- For control tumours, the ratio of necrotic to total volume remains fixed as the tumours grow. For treated tumours this ratio increases with time.

In view of the observations stated above, our aims are: (i) to model the growth of a vascular tumour, explaining the observed spatial structure, and (ii) to understand the effect that adding the drug has on the tumour's development.

Key modelling assumptions

1. The absence of areas of necrosis in the perfused region of the tumour leads us to conclude that angiogenesis occurs everwhere throughout the viable part of the tumour. To understand this, consider the growth of tumour cells between two blood vessels. When the tumour cells proliferate, the local increase in volume causes the two vessels to be pushed apart and the oxygen tension at the midpoint to fall. Transient areas of hypoxia, which produce VEGF, may be created. This local VEGF stimulates new blood vessels to grow into the region and will prevent the appearance of areas of necrosis if the new vessels migrate into the region quickly enough.
2. Microscopic changes in the oxygen tension in the tumour mass between blood vessels can be averaged out. Thus the local average oxygen tension can be characterised by the functional blood vessel density and, thus, "macroscopic hypoxia" is generated when the blood vessel density becomes low. Thus we do not explicitly include oxygen tension as a dependent variable.

Mathematical model describing the growth of control tumours

We assume that the tumour consists of three types of cellular material - live tumour cells, functioning blood vessels and dead matter (primarily necrotic cell debris) and that it grows as a spherically symmetric mass of radius $r = R(t)$. We assume that the mass fraction of tumour cells increases by cell birth (which occurs at a rate proportional to the local mass of cells and the local blood vessel density) and decreases by cell death (at a rate which is proportional to the local cell mass). We assume that the local mass of functional blood vessels increases by angiogenesis, and that this is stimulated by the tumour cells (as described in §3, key point 1). We assume further that the rate at which new blood vessels form is proportional to the local mass of functional blood vessels and to the local tumour cell mass. We suppose that blood vessels become dysfunctional (*i.e.* "die") when the local pressure exceeds some critial pressure, p_{crit}. Finally, we assume that, when tumour cells die, functioning blood vessels instantaneously clear the resulting cellular debris, if the local blood vessel density exceeds a threshold value Y_B^*. If the vessel density falls below this threshold value then the cellular debris is removed at a rate which is proportional to the local vessel density.

We formulate conservation of mass equations for the three mass fractions, namely the mass fraction of live tumour cells, $Y_T(r,t)$, the mass fraction of blood vessels, $Y_B(r,t)$ and the mass fraction of dead material $Y_N(r,t)$. The equations read

$$\frac{\partial Y_T}{\partial t} + \frac{1}{r^2}\frac{\partial}{\partial r}\left(r^2 u Y_T\right) = \underbrace{k_1 Y_B Y_T}_{\text{mitosis}} - \underbrace{k_2 Y_T}_{\text{death}}, \tag{1}$$

$$\frac{\partial Y_B}{\partial t} + \frac{1}{r^2}\frac{\partial}{\partial r}\left(r^2 u Y_B\right) = \underbrace{k_3 Y_B Y_T}_{\text{angiogenesis}} - \underbrace{k_4 Y_B H(p - p_{crit})}_{\text{vessel collapse}}, \tag{2}$$

$$\frac{\partial Y_N}{\partial t} + \frac{1}{r^2}\frac{\partial}{\partial r}\left(r^2 Y_N\right) = \underbrace{k_2 Y_T \left(1 - \frac{Y_B}{Y_B^*}\right) H\left(1 - \frac{Y_B}{Y_B^*}\right)}_{\text{dead material not removed by the vasculature}}. \tag{3}$$

In (1)-(3), $u(r,t)$ and $p(r,t)$ denote the cellular velocity and pressure respectively, p_{crit} denotes the threshold pressure above which the tumour's immature blood vessels become occluded, $k_i\,(i = 1, ..., 4)$ are non-negative rate constants with natural physical interpretations, and Y_B^* is the threshold vessel mass fraction above which all cellular debris is instantaneously cleared via the vasculature.

Two further conditions are needed to determine u and p. Firstly, we assume that there are no voids within the tumour and so we take

$$Y_T + Y_B + Y_N = 1. \tag{4}$$

Secondly, we employ Darcy's Law to provide a constitutive relationship between u and p:

$$u = -\sigma \frac{\partial p}{\partial r}, \tag{5}$$

where the constant σ describes the ease with which cellular material (Y_T, Y_B and Y_N) flows through the tumour's extracellular matrix.

We close the model by specifying the following initial and boundary conditions:

$$u = 0 \qquad \text{at} \qquad r = 0, \tag{6}$$

$$\frac{\partial Y_T}{\partial r} = \frac{\partial Y_B}{\partial r} = \frac{\partial Y_N}{\partial r} = 0 \qquad \text{at} \qquad r = 0, \tag{7}$$

$$p = 0, \qquad \text{at} \qquad r = R(t), \tag{8}$$

$$Y_T(r,0) = T^*(r),\ Y_B(r,0) = B^*(r),\ Y_N(r,0) = 1 - T^*(r) - B^*(r) \quad \text{at} \quad t = 0. \tag{9}$$

Equations (6)-(7) guarantee symmetry of the tumour about its centre, while (8) ensures continuity of pressure across the tumour's surface (at $r = R(t)$). Equations (9) prescribe the initial mass fractions of the tumour cells, blood vessels and necrotis debris.

We note that the position of the tumour radius may be found by solving

$$\frac{\mathrm{d}R}{\mathrm{d}t} = u|_{r=R} \qquad \text{with} \quad R(t=0) = R_{init}. \tag{10}$$

Thus, in summary, our model comprises three hyperbolic partial differential equations (1-3), two constitutive equations (4,5), the 3 boundary conditions (6-8), the initial condition (9) and the equation for the motion of the outer edge of the tumour (10).

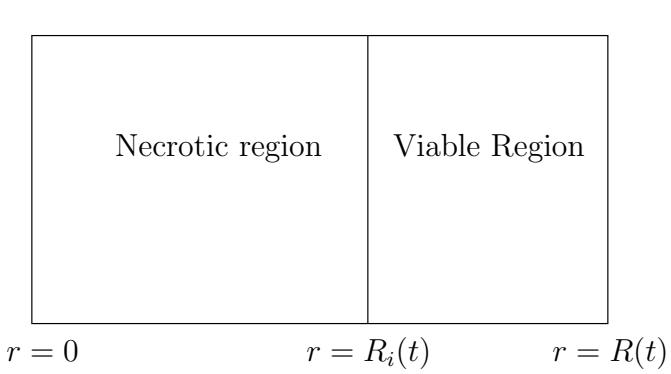

Figure 3: Spatial structure

We nondimensionalise the governing equations using the following scalings

$$t = k_1^{-1} t', \qquad r = R_{init} r', \qquad u = \frac{\sigma p_{crit}}{R_{init}} u', \qquad p = p_{crit} p'. \tag{11}$$

(Note that, since Y_T, Y_B and Y_N are mass fractions, they are already nondimensional quantities.) In this way, we derive the following nondimensional form of equations (1)-(5)

$$\frac{\partial Y_T}{\partial t} + \sigma^* \frac{1}{r^2} \frac{\partial}{\partial r} \left(r^2 u Y_T \right) = Y_T (Y_B - k_2^*), \tag{12}$$

$$\frac{\partial Y_B}{\partial t} + \sigma^* \frac{1}{r^2} \frac{\partial}{\partial r} \left(r^2 u Y_B \right) = k_3^* Y_T Y_B - k_4^* Y_B H(p-1), \tag{13}$$

$$\frac{\partial Y_N}{\partial t} + \sigma^* \frac{1}{r^2} \frac{\partial}{\partial r} \left(r^2 u Y_N \right) = k_2^* Y_T \left(1 - \frac{Y_B}{Y_B^*} \right) H \left(1 - \frac{Y_B}{Y_B^*} \right), \tag{14}$$

$$Y_T + Y_B + Y_N = 1, \tag{15}$$

$$u = -\frac{\partial p}{\partial r}, \tag{16}$$

where $k_i^* = k_i / k_1$ and $\sigma^* = \sigma p_{crit} / k_1 R_{init}^2$. The boundary and initial conditions become

$$u = 0 \qquad \text{at} \qquad r = 0, \tag{17}$$

$$\frac{\partial Y_T}{\partial r} = \frac{\partial Y_B}{\partial r} = \frac{\partial Y_N}{\partial r} = 0 \qquad \text{at} \qquad r = 0, \tag{18}$$

$$p = 0, \qquad \text{at} \qquad r = R(t), \tag{19}$$

$$Y_T(r,0) = T^*(r),\ Y_B(r,0) = B^*(r),\ Y_N(r,0) = 1 - T^*(r) - B^*(r) \quad \text{at} \quad t = 0. \tag{20}$$

$$\frac{\mathrm{d}R}{\mathrm{d}t} = \sigma^* u|_{r=R} \qquad \text{with} \ \ R(t=0) = 1. \tag{21}$$

In order to make analytical progress we suppose that the flow is slow on this proliferation timescale and thus $\sigma^* \ll 1$. Further we set, $k_3^* \sim \sigma^* \ll 1$, since the timescale for blood vessel production (which involves the proliferation, migration and differentiation of a large number of endothelial cells) is much longer than the timescale for the proliferation of live tumour cells. We scale $t = t'/\sigma^*$, to balance the terms in (21), and we seek a solution with the spatial structure shown in Figure 3.

We denote the internal radius at which the pressure is sufficient to occlude the blood vessels by $r = R_i(t)$, (*i.e.* $p = 1$ when $r = R_i(t)$). Thus, any blood vessels located within the central core $r < R_i$ will become

occluded because the pressure there exceeds the threshold level. We seek regular power series expansions for the dependent variables in term of the small parameter σ^* of the form

$$Y_i = Y_i^{(0)} + \sigma^* Y_i^{(1)} + O(\sigma^{*2}), \qquad i = (\mathrm{T},\, \mathrm{B},\, \mathrm{N}), \tag{22}$$

$$u = u_0 + \sigma^* u_1 + O(\sigma^{*2}), \tag{23}$$

$$p = p_0 + \sigma^* p_1 + O(\sigma^{*2}), \tag{24}$$

$$R = R_0 + \sigma^* R_1 + O(\sigma^{*2}). \tag{25}$$

Using (12)-(16), we find that where $p \geq 1$ (*i.e.* $0 \leq r \leq R_i$),

$$Y_T^{(0)} = 0, \qquad Y_B^{(0)} = 0, \qquad Y_N^{(0)} = 1, \tag{26}$$

$$u_0 = 0, \qquad p_0 = 1. \tag{27}$$

Similarly, in the outer region of the tumour, where $p < 1$ and $R_i(t) \leq r \leq R_0(t)$, we have

$$Y_T^{(0)} = 1 - k_2^*, \qquad Y_B^{(0)} = k_2^*, \qquad Y_N^{(0)} = 0. \tag{28}$$

Adding (12)-(14) and equating coefficients of $O(\sigma^*)$, we find that u_0 satisfies

$$\frac{1}{r^2}\frac{\partial}{\partial r}\left(r^2 u_0\right) = \frac{k_3^*}{\sigma^*}(1 - k_2^*). \tag{29}$$

Imposing continuity of u_0 across $r = R_i$ we deduce that

$$u_0 = \kappa_1 r \left(1 - \frac{R_i^3(t)}{r^3}\right), \tag{30}$$

where $\kappa_1 = k_3^*(1 - k_2^*)/3\sigma^*$. Evaluating (30) at $r = R_0(t)$ we find that

$$\frac{\mathrm{d}R_0}{\mathrm{d}t} = u_0|_{r=R_0} = \kappa_1 R_0 \left(1 - \left(\frac{R_i}{R_0}\right)^3\right) \equiv \kappa_1 R_0 (1 - \Phi_i^3), \tag{31}$$

where $\Phi_i = R_i/R_0 \in (0, 1)$. In order to determine the position of the interface $r = R_i$ (or, equivalently $\Phi_i = R_i/R_0$) we now solve for the pressure p_0. Substituting for u_0 into (16), integrating and imposing $p_0 = 0$ at $r = R_0$, we find that

$$p_0 = \kappa_1 \left(\frac{R_0^2}{2} - \frac{r^2}{2} + \frac{R_i^3}{R_0} - \frac{R_i^3}{r}\right). \tag{32}$$

Finally, by noting that $p_0 = 1$ when $r = R_i(t)$, we obtain the following algebraic equation defining $\Phi_i(t)$ in terms of $R_0(t)$:

$$F(\Phi_i) = \Phi_i^3 - \frac{3}{2}\Phi_i^2 + \frac{1}{2} - \frac{1}{\kappa_1 R_0^2} = 0. \tag{33}$$

We remark that in order to obtain physically meaningful solutions of (33) (with $\Phi_i(t) \in [0, 1)$), we require $R_0^2 > 2/\kappa_1$. In this case,

$$F(0) > 0 > F(1), \tag{34}$$

and, thus, providing $R_0^2 > 2/\kappa_1$, there is always a physically relevant solution for which $0 \leq \Phi_i \leq 1$. If $R_0^2 < 2/\kappa_1$, then the pressure is everywhere less than 1 (*i.e.* R_i does not exist), no blood vessels are occluded, there is no necrotic core, and the radius of the tumour grows as

$$R_0 = e^{\frac{\kappa_1 t}{3}}. \tag{35}$$

We note that for large values of R_0, $\Phi_i \to 1$ from below. In fact, for large R_0, equation (33) yields

$$\Phi_i = \frac{R_i}{R_0} \sim 1 - \sqrt{\frac{2}{3\kappa_1}}\frac{1}{R_0} + O\left(\frac{1}{R_0^2}\right). \tag{36}$$

In Figure 4 we use (33) to display the behaviour of R_i/R_0 for $\kappa_1 = 0.1$, 0.5 and 0.9. We note that as κ_1

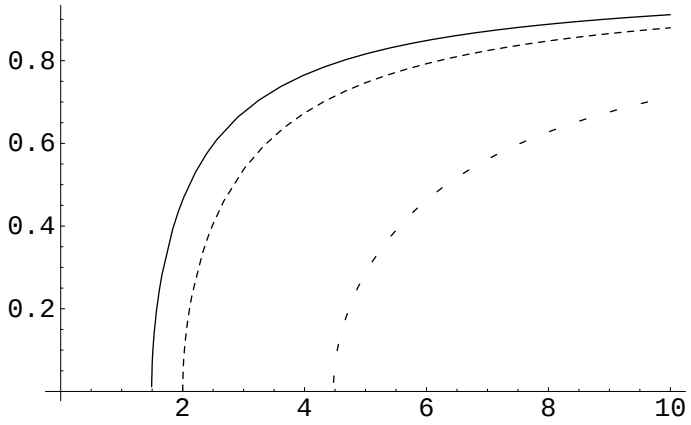

Figure 4: Graph showing how Φ_i varies with R_0, for various values of κ_1: 0.1 - dashed line, 0.5 - dotted line and 0.9 - solid line.

decreases, the size of the tumour at which necrosis is initiated increases. Further, for large R_0, we can see that $\Phi_i \to 1$.

Using (36), we may now determine how $R_0(t)$ evolves. In particular, combining (10) and (30), we find that, for large R_0,

$$\frac{\mathrm{d}R_0}{\mathrm{d}t} = \sqrt{6\kappa_1} \qquad \Rightarrow R_0 \sim \sqrt{6\kappa_1}t. \tag{37}$$

Thus, as R_0 becomes large, the volume of the tumour increases algebraically with time: $V = 4\pi R^3/3 \sim t^3$ as $R_0 \to \infty$. Substituting with R_0 from (37) in (36), we note further that

$$\Phi_i^3 = \left(\frac{R_i}{R_0}\right)^3 = \frac{N}{V} \sim 1 - \frac{1}{3\kappa_1 t} \to 1 \qquad \text{as} \qquad t \to \infty. \tag{38}$$

This prediction does not agree with the experimental observation that $N/V \sim$ constant < 1. However, we note that, post study group, problems in the data were established and the observation that N/V remains constant as the tumours grow may not be true. Thus, we continue to work with this model until new experimental evidence concerning N/V comes to light.

When R_0 is not large, we must solve (31) numerically. For $\kappa_1 > 2$, R_i exists initially and for all time. However, for $\kappa_1 < 2$, there is an initial period in which R_0 grows exponentially (given by (35)), followed by a switch to growth given by (31). We show plots of how the tumour *volume* varies with time, for various values of κ_1, in Figure 5. The changes in the slope of the curves mark the transition to necrotic growth. We see that the tumour grows more quickly as κ_1 increases, and that when R_i does not exist, tumour growth is slow.

We note that we should check that it is possible to match between the "inner" and "outer" solutions presented in this section. We would scale $r = R_i + (\sigma^*)^k\hat{r}$ (for some value of k) and solve the resulting problem in this "boundary layer". We intend to investigate this matching in the future.

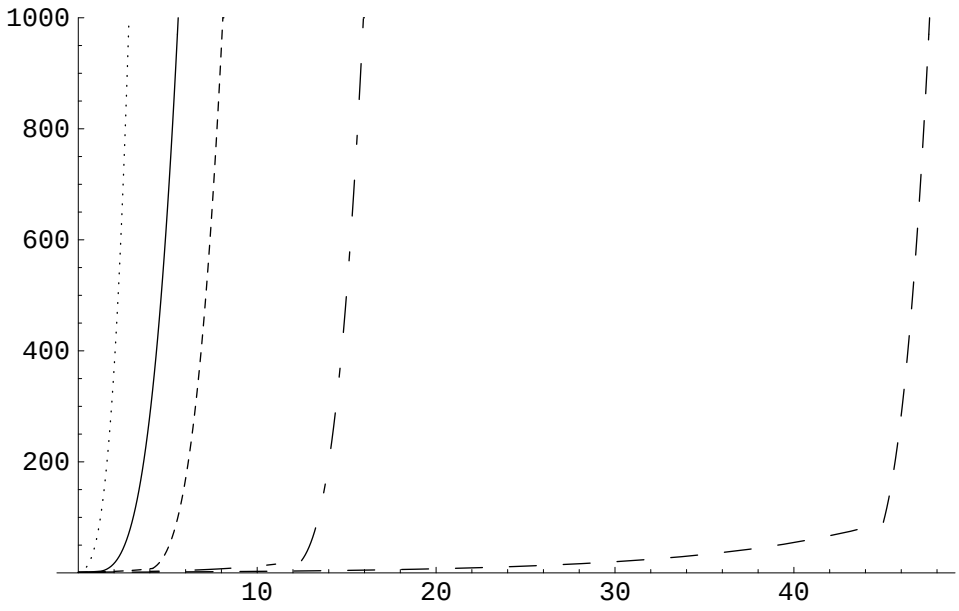

Figure 5: Graph showing R_0^3 against time, for $\kappa_1 = 0.1$ (large dashed line), 0.25 (dot-dashed line), 0.5 (small dashed line), 0.9 (solid line) and 2.1 (dotted line).

Numerical Solution

In this section we present a snapshot of a numerical solution to the model equations (12-16) with boundary conditions (17-21). We select the following parameters:

$$k_2^* = 0.15, \qquad k_3^* = 0.05, \qquad k_4^* = 0.1, \qquad Y_B^* = 0.1, \qquad \sigma^* = 0.05.$$

We show the initial conditions chosen in Figure 6. In this simulation, we choose $R(t = 0) = 2.88$. We note that, in these numerical simulations, we have not scaled $t = t'/\sigma^*$.

In order to solve the mathematical model, we have used smooth-but-steep counterparts to the Heaviside functions. We show the corresponding profiles at $t = 40$ in Figure 7. Finally, we show the change in radius with time in Figure 8. We make the following observations concerning the numerical solutions.

- The initial tumour pressure increases monotonically from zero at the "leading-edge" of the tumour.
- At later times, the tumour pressure has an internal maximum which is close to the leading-edge.
- Both the mass of live tumour cells and the mass of blood vessels have a constant value close to the proliferating edge. The mass of live tumour cells increases from its value at the edge to a plateau value. The mass of functioning blood vessels decreases to a plateau away from the tumour edge.
- There is a drop off from the plateau value to zero in both the mass of live cells and the mass of blood vessels very close to the centre of the tumour, and a corresponding increase in dead material.
- The tumour volume appears to grow as t^3, in line with our earlier asymptotic solution.

We can interpret the solution as follows. In the central region of the tumour, where the masses of blood vessels and live tumour cells remain constant, the solution is found by setting the right hand sides of (12-14)

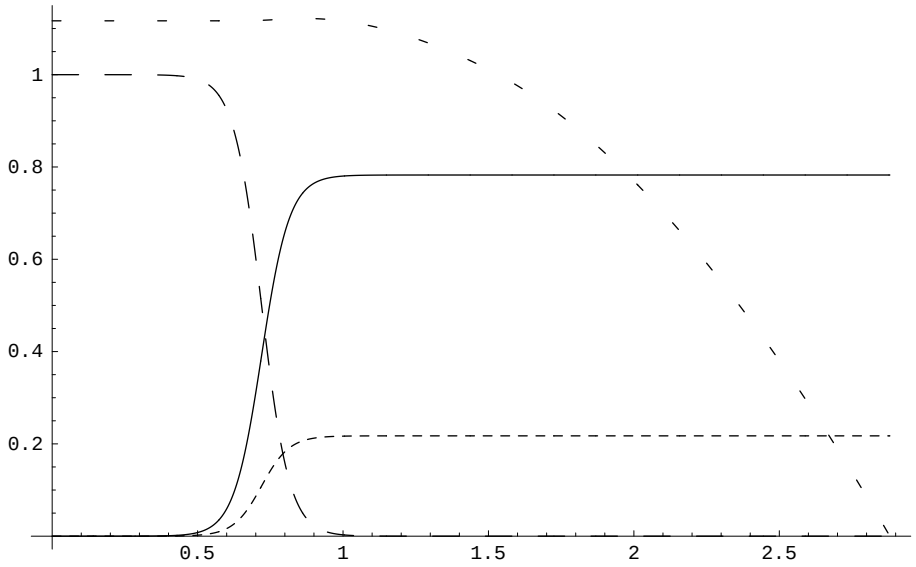

Figure 6: Graph showing the initial conditions for Y_T (solid line), Y_B (close small dashed line), Y_N (large dashed line) and P (spread small dashed line).

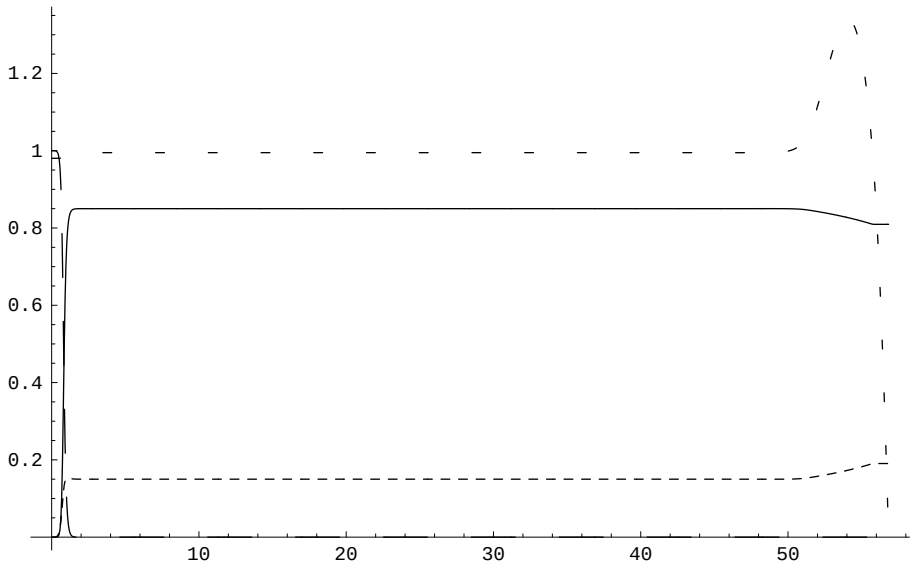

Figure 7: Graph showing Y_T (solid line), Y_B (close small dashed line), Y_N (large dashed line) and P (spread small dashed line) at t=40.

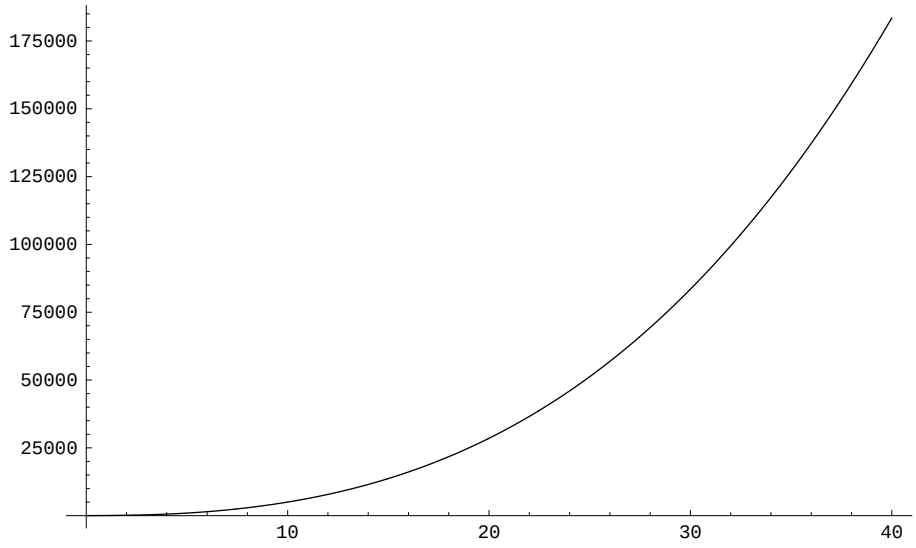

Figure 8: Graph showing how the tumour volume changes with time.

to zero. The solution is given by

$$Y_B = k_2^*, \qquad Y_T = 1 - k_2^*, \qquad Y_N = 0, \qquad \bar{H}(p-1) = \frac{K_3^* Y_T}{k_4^*}, \tag{39}$$

where $\bar{H}$ is the smooth version of the Heaviside function. (Note that this solution then only exists in the case when we replace the heaviside function with its smooth but steep counterpart). At the leading edge, the solution is found by setting $r = R - \sqrt{\sigma^*} r'$, $Y_T = Y_T^* + \sqrt{\sigma^*} Y_T'$, and the solution reads

$$Y_T = \frac{1 - k_2^*}{1 + k_3^*}, \qquad Y_B = \frac{k_2^* + k_3^*}{1 + k_3^*}, \qquad Y_N = 0, \qquad p = \frac{\kappa_1}{2}(R - r)^2 + A(R - r), \tag{40}$$

where A is unknown (and would have to be found by matching). In the central region, all the material is dead (and hence $Y_N = 1$, $Y_T = Y_B = 0$).

We note that there are two further regions within the tumour, the sharp transition zone close to the centre, and the more gentle transition zone close to the leading edge. We can explain why the mass of tumour cells unexpectedly increases in the latter region by considering what is happening there. The end of this region close to the leading edge is the point where P begins to exceed 1. Since, in this model, dead blood vessels occupy no space, when pressure occluded death occurs, Y_B decreases, but Y_N remains at zero. Thus, in order to fill space, the mass of tumour cells must increase. This phenomena is physically incorrect. We would expect that if blood vessels die then the tumour cells surrounding them also die. We discuss altering the model to incorporate these ideas in §.

Mathematical model describing the growth of treated tumours

Having developed and studied a model that describes the growth of a vascular tumour, we now extend it in order to investigate the impact that fibrinogen E fragment (FgnE) has on the tumour's evolution.

We denote by D the nondimensional drug concentration in the bloodstream. We suppose that the drug does not alter the proliferation rate of the blood vessels. Rather, we assume that it causes a dose-dependent

proportion $\phi = \phi(D)$ of the new blood vessels to be dysfunctional *i.e* plugged with fibrinogen. Specifically, we decompose the overall vessel birth rate in (13) into a functioning and a nonfunctioning fraction:

$$\underbrace{k_3^* Y_T Y_B}_{\text{birth rate of new vessels}} = \underbrace{k_3^* Y_T Y_B \phi}_{\text{dysfunctional vessels}} + \underbrace{k_3^* Y_T Y_B (1-\phi)}_{\text{functioning vessels}} . \tag{41}$$

We remark that only the functioning vessels will appear as a source term in equation (13): the dysfunctional vessels are viewed as necrotic material (see below).

Now, FgnE is known to be more potent under low oxygen concentrations. In our model, low oxygen concentrations are equivalent to low functional blood vessel density, and so we assume that FgnE's potency (*i.e.* its ability to produce dysfunctional vessels) is a function of D/Y_B, and we fix

$$\phi(D) = \frac{\frac{D}{Y_B}}{1 + \frac{D}{Y_B}}. \tag{42}$$

Since dysfunctional vessels occupy space but do not supply oxygen, we view them as necrotic matter and modify equations (13) and (14) to read

$$\frac{\partial Y_B}{\partial t} + \frac{\sigma^*}{r^2}\frac{\partial}{\partial r}\left(r^2 u Y_B\right) = k_3^* Y_T Y_B \left(\frac{Y_B}{Y_B + D}\right) - k_4^* Y_B H(p-1), \tag{43}$$

$$\frac{\partial Y_N}{\partial t} + \frac{\sigma^*}{r^2}\frac{\partial}{\partial r}\left(r^2 u Y_N\right) = k_2^* Y_T \left(1 - \frac{Y_B}{Y_B^*}\right) H\left(1 - \frac{Y_B}{Y_B^*}\right) + k_3^* Y_T Y_B \left(\frac{D}{Y_B + D}\right). \tag{44}$$

We remark that equations (12), (15) and (16) are unchanged by the introduction of FgnE into the model. We note also that if $D = 0$ then the original, drug-free model is recovered.

We construct solutions to the model with FgnE using the procedure outlined in section 4. The resulting expressions are identical to those of section 4, with $\kappa_1 = k_3^*(1-k_2^*)/\sigma^*$ replaced by $\kappa_2 = \kappa_1 k_2^*/(k_2^* + D) < \kappa_1$ if $D > 0$.

We now compare the growth of the control (*i.e.* FgnE-free) and treated tumours. In order to do this we recall that for the control tumours ($D = 0$),

$$R_{D=0} \sim \sqrt{6\kappa_1 t} \qquad \text{and} \qquad \left(\frac{R_i}{R}\right)_{D=0} \sim 1 - \frac{1}{3\kappa_1 t}. \tag{45}$$

Similarly, for the treated tumours ($D > 0$),

$$R_{D>0} \sim \sqrt{6\kappa_2 t} \qquad \text{and} \qquad \left(\frac{R_i}{R}\right)_{D>0} \sim 1 - \frac{1}{3\kappa_2 t}. \tag{46}$$

Comparing equations (45) and (46) and noting that $\kappa_2 < \kappa_1$ if $D > 0$, we can see that the treated tumour is smaller that the control tumour. We note also that increasing the drug dose (*i.e.* decreasing κ_2) reduces the tumour's growth rate and, hence, its overall size. Note that we can visualise these changes by considering the curves shown in Figure 9. Here we show how R_0^3 changes with time for various values of κ_2, given that, at $t = 0$, $R = 5$ (*i.e.*, both the treated and untreated tumours are initially the same size, and sufficiently large that they possess a central core of necrosis). We can interpret the upper curve in Figure 9 as a control tumour growth curve, and the two lower curves as treated tumour growth curves. In this way it is easy to see that the tumour's growth rate is retarded by the addition of the drug. By considering the nondimensionalisation process used to rescale the model equations, we can also compare the predictions of the mathematical model with the experimental data presented in Figure 1. We rescale time with $1/k_1$ (where k_1 = tumour cell

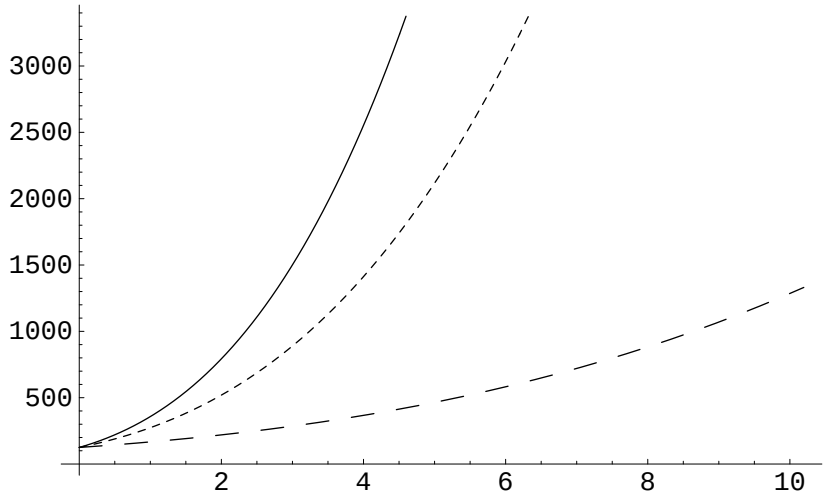

Figure 9: Graph showing R_0^3 against time, for $\kappa_2 = 0.1$ (large dashed line), 0.5 (small dashed line) and 0.9 (solid line).

proliferation rate) and then rescaled with $1/\sigma^*$. If we suppose that $k_1 = 2$ day^{-1} and $\sigma^* = 0.05$, we find that $t_{dim} = t_{nondim}/(k_1\sigma^*) = 10t_{nondim}$. Thus 1 dimensionless time unit equates to 10 days. Referring to Figure 9 we note that on this timescale the tumour grows approximately linearly, and that this is in good qualitative agreement with the data presented in Figure 1.

We now investigate how the proportion of the tumour that is necrotic depends on the drug dose, D. From (45) and (46) we find

$$\frac{(R - R_i)^3_{D>0}}{(R - R_i)^3_{D=0}} = \left(\frac{\kappa_1}{\kappa_2}\right)^{3/2} > 1. \tag{47}$$

Thus, our model predicts that the treated tumours have *larger* proliferating areas than control tumours. This result is *not* supported by the experimental observations.

Model Modifications and Extensions

In this section we discuss several ways in which our model could be modified in order to obtain better agreement with the experimental observations.

Choice of Constitutive Law Governing Cell Motion

Our original choice of consitutive law was motivated by the paper of Greenspan (and a number that followed it). However, "Darcy's law", which adequately describes fluid flow through a porous medium, is not necessarily the correct consitutive relationship to describe the flow of cells through extracellular matrix. A natural alternative would be to treat the cells as a viscous liquid. In this case the expression linking u and p given by (5) would be superceded by the conservation of momentum equation (the Navier-Stokes equation) for a viscous fluid. Taking care to remember that the liquid is "compressible" (*i.e.* that $\nabla.u \neq 0$), we would set

$$-\frac{\partial p}{\partial r} + \mu\left(\frac{1}{r^2}\frac{\partial}{\partial r}\left(r^2\frac{\partial u}{\partial r}\right) - \frac{2u}{r^2} + \frac{1}{3}\frac{\partial F(r)}{\partial r}\right) = 0, \tag{48}$$

where

$$\frac{1}{r^2}\frac{\partial}{\partial r}(r^2 u) = F(r), \tag{49}$$

μ denotes the coefficient of viscosity, and $F(r)$ is the sum of the source and sink terms from (1-3), and reads

$$F(r) = [(k_1 + k_3)Y_B - k_2]Y_T - k_4 Y_B H(p - p_{crit}) + k_2 Y_T \left(1 - \frac{Y_B}{Y_B^*}\right) H\left(1 - \frac{Y_B}{Y_B^*}\right). \tag{50}$$

When (48) is used in place of (5) the control and treated tumour solutions presented in sections 4 and 6 still apply, apart from the pressure field. Substituting for u_0 from (30) and solving (48), we find that

$$p_0 = \text{constant} = 0. \tag{51}$$

Thus, there is no build up of pressure in the viable part of the tumour mass, and thus this model is not appropriate.

A further extension of the model could be to assume that the three phases (T, B, N) move with different speeds. We would envisage modelling the live tumour cells as a material which exhibited both viscous and elastic properties (since we can see that viscous alone will not work), the blood vessels as another material exhibiting viscous and elastic properties, and dead matter as an inviscid liquid (*i.e.* moving via a modified Darcy's law).

Other source and sink terms

There are numerous alternatives for the source and sink terms in equations (1)-(3). Here we mention in passing several possible modifications.

1. Effects due to the formation of dysfunctional vessels.

   There are several logical modifications that we could make to our model which involve better descriptions of the "death" of blood vessels. At present, blood vessels killed by pressure occlusion occupy no mass within the tumour, and also the death of a blood vessel only indirectly affects the local density of tumour cells. Thus, it would be better to explicitly provide for an increase in cellular death due to blood vessel collapse, and to take account of the mass of dysfunctional vessels by including them in the dead cell phase. Thus we propose modifying the source-sink terms in (1) and (3) to read

$$Q_T = k_1 Y_B Y_T - k_2 Y_T - k_6 Y_T H(p - p_{crit}), \tag{52}$$

$$Q_N = (k_2 + k_6 H(p - p_{crit}))Y_T \left(1 - \frac{Y_B}{Y_B^*}\right) H\left(1 - \frac{Y_B}{Y_B^*}\right) + k_5 Y_B H(p - p_{crit}). \tag{53}$$

   We note that the effect of including the increase in cellular death due to vessel collapse is identical to allowing the proliferation rate k_1 to vary spatially within the tumour.

2. Effects due to presence of the drug.

   Our drug, at present, causes a proportion of the blood vessels born to be clogged and thus be dysfunctional. It is also possible that the drug changes the functional blood vessels, reducing their ability to clear away dead material, for example. We would model such an effect by making Y_B^* increase with drug concentration, replacing Y_B^* with $Y_B^*(1 + D)$ for example.

Conclusions

We have presented a model to describe the growth of a vascular tumour, in the presence and absence of fibrinogen E fragment (FgnE). When there is no drug present, our model admits a solution with the observed

spatial structure, that is, a central necrotic region surrounded by a region containing viable tumour cells and functioning blood vessels. In the outer region the blood vessel density remains constant as the tumour grows. For large times, we predict that the tumour volume increases in proportion to t^3.

When the tumours are treated with FgnE, our model predicts that they will have smaller radii than the control tumours, and that the reduction is size will increase with increasing dose. These predictions are in good agreement with the experimental observations.

We have been unable to capture the observations that the ratio of the necrotic volume to the total volume remains constant in the control tumours and increases with time in the treated tumours. However, doubt has been cast on this piece of experimental evidence and we wait to see whether it is true.

We have presented details of the ways in which we plan to modify the model in the future.

Acknowledgements

Report submitted by C Breward and H Byrne. The numerical solutions in §5 were computed by E Clark. Workshop contributions from J Billingham, C Breward, H Byrne, SJ Chapman, E Clark, S Franks, E Gaffney, D Gammack, P Howell, A King, J King, P Kramer, C Lewis, J Norbury, M Owen, C Please, M Tindall, J Ward and D Wilson.

References

1. C.A. Bootle-Wilbraham, S. Tazzyman, J.M. Marshall and C.E. Lewis (2000). Fibrinogen E-fragment inhibits the migration and tubule formation of human dermal microvascular endothelial cells *in vitro*. *Cancer Research* **60**, 4719-4724.

2. H.P. Greenspan (1976). On the growth and stability of cell cultures and solid tumours. *J. Theor. Biol.* **56**, 229-242.

3. J.P. Ward and J.R. King (1997). Mathematical modelling of avascular tumour growth. IMA J. Math. Appl. Med. **14** 39-69.